Climate, topography and soil factors interact to drive community trait distributions in global drylands

Yoann Le Bagousse-Pinguet[1,2†*], Pierre Liancourt[3†*], Nicolas Gross[2,4,5†*], Francesco de Bello[1,3], Carlos Roberto Fonseca[6], Jens Kattge[7,8], Enrique Valencia[2], Jan Leps[1,9], Fernando T. Maestre[2]

[†] Equal contribution of the authors to this work

[1]Department of Botany, University of South Bohemia, Na Zlate stoce 1, 370 05 Ceske Budejovice, Czech Republic, *[2]Departamento de Biología y Geología, Física y Química Inorgánica, Escuela Superior de Ciencias Experimentales y Tecnología, Universidad Rey Juan Carlos, C/ Tulipán s/n, 28933 Móstoles, Spain,* *[3]Institute of Botany, Czech Academy of Sciences, Dukelská 135, 379 82 Trebon, Czech Republic,* *[4]INRA, USC1339 Chizé (CEBC), F-79360, Villiers en Bois, France,* *[5]Centre d'étude biologique de Chizé, CNRS - Université La Rochelle (UMR 7372), F-79360, Villiers en Bois, France,* *[6]Departamento de Ecologia, Universidade Federal do Rio Grande do Norte, Natal, 59072-900 RN, Brazil,* *[7]Max Planck Institute for Biogeochemistry, Hans Knoell Str. 10, 07745 Jena, Germany,* *[8]German Centre for Integrative Biodiversity Research (iDiv) Halle-Jena-Leipzig; Deutscher Platz 5e; 04103 Leipzig,* *[9]Institute of Entomology, Biology Centre CAS, 370 05 Ceske Budejovice, Czech Republic*

* *Correspondence authors. E-mails:* y.b-pinguet@orange.fr, pierre.liancourt@gmail.com, Nicolas.GROSS@cebc.cnrs.fr

Total number of word: 6023, Main Body: 4086, Abstract: 261, references: 46

Abstract

The skewness and kurtosis of community trait distributions (CTDs) can provide important insights on the mechanisms driving community assembly and species coexistence. However, they have not been considered yet when describing global patterns in CTDs. We aimed to do so by evaluating how environmental variables (mean annual temperature [MAT] and precipitation [MAP], precipitation seasonality [PS], slope angle and sand content) and their interactions affected the mean, variance, skewness, kurtosis of the plant CTDs in global drylands. We gathered specific leaf area and maximum plant height data from 130 dryland communities from all continents except Antarctica. Over 90% of the studied communities had skewed CTDs for SLA and height or had kurtosis values differing from those of normal distributions. Higher MAT and/or lower MAP led to a shift toward plant communities over-represented by "conservative" strategies, and a decrease in functional diversity. However, considering interactions among environmental drivers increased the explanatory power of our models by 20%. Sand content strongly altered the responses of height to changes in MAT and MAP (climate × topo-edaphic interactions). Increasing PS reversed the effects of MAT and MAP (climate × climate interactions) on the four moments of CTDs for SLA, particularly in dry-subhumid regions. Our results indicate that the increase in PS forecasted by climate change models will reduce the functional diversity of dry-subhumid communities. They also indicate that ignoring interactions among environmental drivers can lead to misleading conclusions when evaluating global patterns in CTDs, and thus may dramatically undermine our ability to predict the impact of global environmental change on plant communities and associated ecosystem functioning.

Keywords: arid systems, functional biogeography, maximum plant height, precipitation regimes, sand content, slope, specific leaf area, temperature.

INTRODUCTION

Community trait distributions (CTDs) are the frequency patterns of trait values weighted by the species abundance observed in communities (Violle et al. 2007). They can be used to make accurate prediction of plant species distributions (Frenette-Dussault et al. 2013), to assess plant community responses to environmental gradients (Soudzilovskaia et al. 2013), and to quantify ecosystem stability under varying environmental conditions (Valencia et al. 2015). Therefore, evaluating patterns of CTDs along biogeographic gradients is a powerful tool to predict the impact of climate change on communities and ecosystems (Violle et al. 2014, Enquist et al. 2015), particularly at the global scale (Parmesan et al. 2013).

Ongoing climate change involves simultaneous shifts in multiple environmental factors, such as temperature and precipitation regimes (IPCC 2013). These variables are expected to interact in a complex way to determine their impacts on plant communities and ecosystem functioning (see Peñuelas et al. 2013 for a review). For instance, concomitant effects of annual amount and seasonality of precipitations can equally affect aboveground net plant productivity (Guo et al. 2012). Additionally, plant community responses to altered temperature and precipitations regimes can also be conditional on local topography (Liancourt et al. 2013) and soil parameters (e.g., Fridley et al. 2011). To date, regional patterns of CTDs have been assessed along isolated climatic (Fonseca et al. 2000, Freschet et al. 2011, Laughlin et al. 2011, Swenson et al. 2012) or edaphic gradients (e.g., Fonseca et al. 2000, Gross et al. 2008). However, global patterns of CTDs in response to interacting environmental factors are barely known. Therefore, understanding how interactions between environmental factors determine global patterns of CTDs can substantially advance our understanding of the complex effects of climate change on plant functional diversity and ecosystem functioning.

Studies quantifying patterns of CTDs have mostly targeted the community-weighted mean (e.g., Gross et al. 2008, Laughlin et al. 2011), which focuses on the traits of the most

dominant species, and the community-weighted variance (or related indices, e.g., Freschet et al. 2011, Swenson et al. 2012), which measures the general extent of functional diversity in a community. While the mean and variance of CTDs suffice to characterize normal distributions, CTDs are often non-normal and sometimes even multimodal (Fonseca et al. 2000, Enquist et al. 2015). In such cases, the skewness and kurtosis of CTDs complement the information provided by the mean and variance by providing insights on the mechanisms determining community assembly and species coexistence (Schamp et al. 2008, Kraft et al. 2008, Enquist et al. 2015; Fig. 1). Swenson and Weiser (2010) found that the skewness and kurtosis of CTDs from Eastern North American trees were highly sensitive to temperature and precipitation. Their results highlight the importance of their investigation in a context of functional biogeography and global environmental change.

Drylands, including arid, semi-arid and dry-subhumid ecosystems, cover ~41% of Earth's land surface and support over 38% of the total global population (Safirel and Adeel 2005), and are particularly sensitive to climate change (see Maestre *et al.*, 2012a for a review). Despite their importance, no study so far has simultaneously considered the interactive effects of climate, topography and soil factors on the four moments of the traits distributions in global drylands. We aimed to do so by assessing specific leaf area (SLA) and maximum plant height of perennial vegetation in 130 dryland communities worldwide, which encompass the major abiotic features and vegetation types found in drylands globally (Appendix S1). Specific leaf area is a key trait indexing leaf-level carbon gain strategies (leaf "economics"; Wright et al. 2004). Maximum plant height reflects a trade-off for biophysical constraints in determining water fluxes within the plant (Enquist 2002), and is related to competitive ability (Westoby 1998). Specific leaf area and maximum plant height reflect two important independent axes of plant ecological strategy (Westoby 1998), and are sensitive to both climatic (e.g., Wright et al. 2004) and edaphic (e.g., Fonseca et al. 2000) variables. In

drylands, these traits can help to explain species coexistence and the dominance of particular plant strategies (e.g. stress-tolerant vs. stress avoidant: Fonseca et al. 2000, Frenette-Dussault et al. 2012, Gross et al. 2013). Along a regional aridity gradient, changes in CTDs of the two studied traits have been shown to impact the strength of biotic interactions (Gross et al. 2013), and the stability of ecosystem multifunctionality (Valencia et al. 2015).

Following the environmental filtering hypothesis (Keddy 1992), we predict that (i) higher environmental stress will lead to a shift toward plant communities over-represented by short species with "conservative" strategies. A decrease in the mean and/or an increase in the skewness for height and SLA with environmental stress will reflect this functional shift. Additionally, we expect (ii) either a decrease in functional diversity due to environmental stress (lower variance and/or higher kurtosis) or an increase in functional diversity due to a decrease in the importance of competitive interactions (higher variance and/or lower kurtosis). Finally, we forecast that (iii) the interactions between climate, topography and soil factors will strongly influence the four moments of CTDs.

MATERIALS AND METHODS

Study sites and environmental variables

Field data for this study were obtained from 130 sites located in 13 countries (Argentina, Australia, Chile, China, Ecuador, Israel, Kenya, Mexico, Morocco, Spain, Tunisia, USA and Venezuela; Fig S1). These sites are a subset of the global network of sites from Maestre et al. (2012b) that cover a wide range of the environmental conditions found in global drylands (excluding hyper arid areas, which usually have little or no perennial vegetation). Mean annual temperature (MAT) and mean annual precipitation (MAP) of the studied sites varied between -1.8°C to 27.8°C, and from 79 mm to 1177 mm, respectively. Slope values ranged

between 0.2° and 28°. The sites studied include a wide variation in soil types, with more than 25 different categories from the FAO´s classification (FAO 1998).

Site climate was summarised using three variables: mean annual temperature (MAT), mean annual precipitation (MAP) and precipitation seasonality (PS: coefficient of variation of 12 monthly rainfall totals). We selected these variables because: i) their measurement is unambiguous; ii) they are important drivers of trait variation both at regional and global scales (e.g., Wright et al. 2004, Swenson et al. 2012, Moles et al. 2014); iii) they are key variables for explaining global variation in dryland ecosystem functioning (Maestre et al. 2012b); and (iv), MAT, MAP and PS describe largely independent features of site climate in the studied dataset (bivariate correlations, $r < 0.36$ in all cases, Appendix S2). Temperature seasonality (standard deviation * 100) was not considered due to its correlation with MAT in the studied dataset ($r = 0.59$). Standardized climate data for all study sites were obtained from Worldclim (www.worldclim.org), a high resolution (30 arc seconds or ~ 1km at equator) global database (Hijmans et al. 2005).

Topo-edaphic variables (i.e. soil properties and topography) at each site were summarised using slope angle and soil sand content. These variables are particularly interesting in the context of this study because they can largely affect moments of CTDs such as community-weighted mean and variance (Dubuis et al. 2013), and because they play key roles in controlling infiltration, water and nutrient availabilities and run-on/run-off processes in drylands (e.g., Gómez-Plaza et al. 2001). Sand, clay and silt contents were measured in soil samples (0-7.5 cm depth) from under the canopy of the dominant perennial plants, and in open areas devoid of vascular vegetation, corresponding to the main microsites present at each site (see Maestre et al. 2012b for details). Soil pH was measured with a pH meter, in a 1: 2.5 mass: volume soil and water suspension. Site-level estimates for all variables were obtained by using the average of the mean values observed in bare ground and vegetated

areas, weighted by their respective area at each site (Maestre et al. 2012b). We did not consider soil pH in further analyses due to its correlation with MAP and sand content (r = -0.62 and -0.53, respectively). Similarly, clay and silt contents were not used in our analyses due to their correlation with sand content (r = -0.52 and -0.55, respectively). Slope at each site was quantified by direct measurements *in situ* with a clinometer.

Community trait distributions

Community trait distributions were estimated by merging two independent datasets. The cover of each perennial plant species measured *in situ* was used as a proxy of species abundance. SLA and maximum plant height were retrieved from the TRY database (Kattge et al. 2011). Site selection was based on the availability of trait data. A site was selected when SLA and plant height data were available for all the perennial species that accounted together for at least 60% of the total perennial vegetation cover (Appendix S3). In total, 130 sites were selected, providing SLA and maximum plant height data for 347 and 512 species, respectively. We also repeated our analyses using a subset of 95 sites for which SLA and plant height data were available for all the perennial species that accounted together for at least 80% of the total perennial vegetation cover at each site, a threshold recommended when estimating CTDs (Pakeman and Quested 2007). Results from this subset of data were consistent with those based on the dataset used with the 60% threshold (Appendix S4), and thus will not be presented in the main text.

For each of the 130 studied sites, community-weighted mean, community-weighted variance, community-weighted skewness and community-weighted kurtosis were computed using the R functions of Bernard-Verdier et al. (2012). In the case of non-normal CTDs, differences in the degree of skewness highlight a shift in the dominance of species with trait values toward one of the extreme of the trait range in a given community (Fig. 1). This pattern may arise from abiotic filtering selecting for a particular set of extreme trait values (Keddy

1992), from biotic filtering such as asymmetric light competition among species (Schamp et al. 2008), the importance of rare species in local co-existence or time lags in community responses to rapid environmental changes (Enquist et al. 2015). Kurtosis highlights the level of trait differentiation between co-occurring species (similar to the trait spacing in Kraft et al. 2008). High kurtosis is characteristic of peaked CTDs, and reflects the occurrence of strong environmental filtering. Low kurtosis is characteristic of flat CTDs, reflecting multiple community assembly processes, or the occurrence of stabilizing niche differences among interacting species (Chesson 2000). Very low kurtosis is characteristic of bimodal CTDs. Bimodal CTDs arise from multiple optimal trait values reflecting either the co-existence of contrasting functional strategies (Gross et al. 2013), or the co-occurrence of past and present optimal trait values in response to recent environmental changes (Enquist et al. 2015).

Statistical analyses

We first built separate linear regression models for each moment of CTDs (mean, variance, skewness and kurtosis) for SLA and height using the five selected environmental variables as predictors (MAT, MAP, PS, slope and sand content) without interactions. Correlation among the predictors used, and thus multicollinearity, was low (r < 0.39 and Variance Inflation Factor [VIF] <1.25 in all cases, Appendix S2). Latitude and longitude were also included in all models to account for potential effects of spatial autocorrelation between sites (Maestre et al. 2012b). Correlation between geographical and studied environmental variables was also low (r < 0.33 and VIF < 1.44 in all cases, Appendix S2). Then, we ran a second set of analyses where all possible two-way interactions between MAT, MAP, PS, slope and sand content were included in the models. For each trait and moment, we used a backward-forward stepwise regression procedure to select the models that minimized the second-order Akaike information criterion (AICc).

We evaluated the relative importance of the predictors considered and their interactions as drivers of the variation found for each trait and moment using a variance decomposition analysis based on the best model selected (see Dubuis et al. 2013 for a similar approach). First, the variance decomposition was used to highlight the percentage of variance explained by the interactions among predictors. Thus, the following five identifiable variance fractions were disentangled: i) latitude and longitude, ii) MAT, MAP and PS, iii) slope and sand content, iv) interactions among predictors and v) unexplained variance. Second, the variance decomposition was used to highlight the percentage of variance explained by climate (and their interactions), topo-edaphic (and their interactions) and climate × topo-edaphic interactions. Thus, the following seven identifiable fractions of variance were disentangled: i) latitude and longitude, ii) climatic variables, iii) climate × climate interactions, iv) local topo-edaphic variables (slope and sand content), v) topo-edaphic × topo-edaphic interactions, vi) climate × topo-edaphic interactions and vii) unexplained variance.

Finally, we conducted a sensitivity analysis of the selected models to illustrate how climate × climate and climate × topo-edaphic interactions drive variations in CTDs in the studied drylands. For doing so, we used the parameter estimates of the climatic and topo-edaphic variables obtained from the best models (based on AICc). Other variables included in these best models were treated as constants and fixed to their mean. Predicted values were obtained by fixing one of the two interacting predictors both at the lowest and highest values observed in the dataset.

All statistical analyses were performed using the R statistical software 2.15.1 (R Core Team 2012). All response variables (community-weighted moments) were log-transformed, and all the predictors (climatic and topo-edaphic variables) were standardized and normalized (z-score) before analyses.

RESULTS

Most of the CTDs did not follow a normal distribution, highlighting the relevance of the use of skewness and kurtosis in evaluating change in CTDs (Appendix S5). Among the 130 studied communities, over 90% of the CTDs for SLA and height were skewed (skewness < -1 or > 1) or had kurtosis values differing from those of normal distributions (kurtosis < -1 or > 1). Furthermore, more than 53% of the CTDs for SLA and height were highly skewed (skewness < -2 or > 2) or had a kurtosis highly departing from that characterizing normal distributions (kurtosis < -2 or > 2).

Additive effects of climate soil and topographic factors on CTDs

When interactions among predictors were not included in the models, the predictive power of the models was relatively modest, and decreased for skewness and kurtosis (Table 1). Climatic variables were always significant predictors for all moments and traits evaluated (Table 1), explaining up to 27% of the total variance for SLA (Fig. 2a: variance) and up to 18% for height (Fig. 2b: mean). Topo-edaphic variables explained less than 4% of the total variance in all cases (Table 1).

Higher MAT simultaneously decreased the mean and variance for SLA and increased kurtosis (Table 1), reflecting a shift from flat and wide spread or even bimodal distributions, dominated by high SLA values, to narrow and peaked trait distributions dominated by low SLA. In contrast, higher MAP increased the mean and decreased the skewness for SLA, apparently leading to skewed distributions dominated by high SLA values. Higher MAP was also associated with increased variance for SLA, reflecting wide spread distributions. Finally, higher sand content was also associated with trait distributions dominated by low mean SLA (Table 1), with flat, wide spread or even bimodal distribution (low kurtosis).

Higher MAT and slope angle values increased the mean and kurtosis for height (Table 1), reflecting changes in trait distributions toward peaked CTDs dominated by tall species. In

contrast, higher MAP led to skewed and peaked trait distributions for height (high skewness and kurtosis), i.e., communities over-represented by relatively small species. Both mean and variance for height decreased with increases in PS, indicating changes toward narrow trait distributions dominated by small species.

Interactive effect of climate, soil and topographic factors on CTDs

Including interactions among predictors substantially increased the predictive power of the models (Table 1). Interactions between MAT and PS, and between MAP and PS (Table 1), explained a large part of the variation in SLA (Fig. 2c: climate × climate interactions). At low values of PS, MAT and MAP increased the mean and variance for SLA, and decreased its skewness (Fig. 3a, c and e). This reflected changes in CTDs toward left-skewed and widespread distributions dominated by species with high SLA values. In contrast, large PS values strongly dampened, and even reversed the effect of MAT and MAP (Fig. 3b, d anf f). Narrow distributions (low variance) dominated by species with low SLA values (low mean and right-skewed) occurred under higher MAT and MAP conditions.

Interactions between MAT and sand content, and between MAP and sand content, explained a large part of variation for height (Table 1, Fig. 2d: climate × topo-edaphic interactions). These results indicate that sand content mediates the effect of climate on CTDs. For instance, CTDs were primarily dominated by short species (Fig 4a and e) but were bimodal (Fig. 4g) at low levels of sand content under high MAT and low MAP. At high level of sand contents, and under similar MAT and MAP conditions, CTDs were dominated by the tallest species (Fig. 4b), and were unimodal (Fig 4h).

DISCUSSION

Community trait distributions (CTDs) in global drylands are highly sensitive to climatic variables such as MAT and MAP. Following our first two hypotheses, environmental stress

(i.e. higher MAT and/or lower MAP values) leads to plant communities over-represented by "conservative" strategies and a decrease in functional diversity. However, climate × climate interactions largely explain variations in CTDs of global drylands, and topo-edaphic variables mediate the effect of climate on the four moments (climate × topo-edaphic interactions), consistently with our third hypothesis. Precipitation seasonality reverses the effects of mean temperature and precipitation on CTDs for SLA. Similarly, soil parameters such as sand content determine the effect of MAT and MAP on plant community height. Importantly, the CTDs of most of the studied communities strongly departed from normal distributions, which highlight the need for detailed analyses of skewness and kurtosis.

Additive effects of climate, soil and topographic factors on CTDs

The effects of climate on the mean of the CTDs for SLA and maximum plant height are consistent with other global studies conducted at the species level (e.g., Wright et al. 2004, Reich et al. 2007, Moles et al. 2014). Higher MAT decreased the mean SLA and increased the height of communities (Soudzilovskaia et al. 2013, Moles et al. 2014), reflecting a decrease in abundance of herbaceous perennial vegetation relative to the abundance of shrubs with evergreen leaves in warmer drylands. Such functional shifts have been documented in the Chihuahuan Desert, and have been attributed to recent climate warming (Brown et al. 1997). Interestingly, functional shifts toward higher abundances of evergreen shrubs have also been observed in response to experimental climate warming in colder biomes (e.g., Walker et al. 2006).

Higher MAP led to communities with increased average SLA values. Communities occurring in the wettest part of the precipitation range studied (i.e. sub-humid drylands) are dominated by species with exploitative strategies, with potential for relatively quick returns on investments of nutrient and dry mass in leaves (Fonseca et al. 2000, Wright et al. 2004). Soil characteristics and topography had much lower explanatory power than climatic

variables as predictors of variations in SLA and maximum height, and only slightly drove variations in the distributions of both traits. Soil texture is an important abiotic filtering that selects for particular set of trait values (e.g., Keddy 1992), i.e. slow-growing perennial vegetation (or evergreen habit). Such a functional shift likely occurs because high sand content is typically found in sites with low nitrogen contents within the sites studied (Maestre et al. 2012b, Delgado-Baquerizo et al. 2013).

Skewness and kurtosis of CTDs were highly sensitive to climate, soil and topography. Higher MAT led to peaked or narrow distributions for SLA and height, reflecting a loss of functional diversity due to the strong effect of abiotic filtering (Keddy 1992). In contrast, flat and even bimodal distributions for SLA occurred for communities in cooler conditions, reflecting an increase in the importance of competitive interactions (Gross et al. 2013).

Higher MAP increased the over-representation of short species with relatively high SLA, co-occurring with rare tall species with low SLA (i.e. a shift toward right-skewed distributions for height and left-skewed distributions for SLA). This over-representation in high SLA may reflect a direct response to a more favorable environment. Alternatively, it may also reflect the occurrence of positive interactions between tall stress-tolerant and exploitative stress-intolerant species. Gross et al. (2013) found that, at low aridity levels, conservative tall species can facilitate the persistence of short fast-growing species that do not tolerate water stress in Mediterranean shrublands.

Interactive effects of climate, soil and topographic factors on CTDs

Considering interactions among environmental drivers strongly increased the explanatory power of our models. Thus, our findings highlight the importance of considering these interactions when assessing large-scale patterns of CTDs. Until now, both climate × climate and climate × topo-edaphic interactions have received very little attention when exploring the drivers of variations in functional traits at both species and community levels (see Reich et al.

2007 for climate × climate interactions, Ordonez et al. 2009 for climate × topo-edaphic interactions). While considering effects of environmental variables as additive (without interactions) can allow capturing general biological trends of large-scale patterns of CTDs (e.g., Freschet et al. 2011, Swenson and Weiser 2010, Swenson et al. 2012), conclusions drawn from such analyses could be misleading, and may dramatically undermine our ability to predict the impact of global environmental change on plant community structure and associated ecosystem functioning.

The importance to consider interactions between environmental drivers is clearly illustrated by the effect of precipitation seasonality, which reversed the effects of MAT and MAP on SLA (Fig. 3). Climate warming is expected to spatially and temporally alter precipitation regimes, and to trigger complex interactive influences on diversity (see Peñuelas et al. 2013 for review). Our results indicate that an increase in PS can particularly affect drylands with warm and relatively wet climate, such as the dry-subhumid regions of our dataset (e.g., Ecuador and Venezuela). Under low seasonality, dry-subhumid ecosystems are dominated by communities with relatively fast-growing and water stress-intolerant vegetation (high SLA), and harbor a high functional diversity. Increasing seasonality can strongly affect the functional structure of these communities by increasing the dominance of slow-growing species and thus reducing their functional diversity. This finding is particularly important because dry-subhumid regions are facing altered seasonal climatic patterns due to ongoing climate change which will likely increase the degree of drought stress they will experience in the future (IPCC 2013).

Sand content altered the height responses to changes in MAT and MAP, highlighting the importance to also consider edaphic factors to forecast the effect of climate change on plant communities (Fridley et al. 2011, Liancourt et al. 2013). Small and tall species tend to co-occur within communities under high MAT and low MAP conditions (bimodal trait

distributions for height). Bimodal distributions for height reflect the structure of perennial dryland vegetation characterized by patches of tall shrubs co-occurring with small species (e.g., Australian woodlands; Eldridge 1999). However, an increase in sand content can alter the functional structure of those communities by selecting for tall species only (unimodal trait distributions for height). The support of taller and denser perennial vegetation on coarse (sandy) soils than on finer-textured soils is a commonly observed pattern in arid and semi-arid climates, generally referred as “inverse texture effect” (Noy Meier 1973).

Finally, it is interesting to notice that latitude and longitude explained a large part of the variation found in our data, and drove the overall decrease in explanatory power for the higher moments of the trait distribution. While our dataset did not allow us to explore the role of these geographic variables (they were not correlated with the studied environmental variables), their predictive power on CTDs is intriguing, and calls for further studies to identify their biological meaning. Latitude and longitude are increasingly used to assess patterns in functional biogeography (e.g., Swenson et al. 2012), and they likely reflect non-considered sources of variations associated to geography in our study. They may encompass differences in species pool, solar irradiance, soil variables not measured here or land-use patterns and history, which are all likely to affect CTDs.

Conclusions

Our study illustrates how trait-based approaches that consider the four moments of the CTDs, reveals the signature of ecological processes at large scales. It has ramifications for improving our predictions on the effect of climate change on plant communities (Violle et al. 2014) and on ecosystem functions (Enquist et al. 2015). This approach would certainly gain predictive power by integrating intraspecific trait variations, and particularly by considering complex shapes of individual-level trait distributions (Laughlin et al. 2015).

ACKNOWLEDGEMENTS

We specially acknowledge all the member of the EPES-BIOCOM network for their contribution to the global dryland database used. This research was supported by the European Research Council under the European Community's Seventh Framework Programme (FP7/2007-2013)/ERC Grant agreement 242658 (BIOCOM). Y.L.B.P. is supported by the project Postdoc USB (reg.no. CZ.1.07/2.3.00/30.0006) realized through EU Education for Competitiveness Operational Programme. This project is funded by European Social Fund and Czech State Budget. Y.L.B.P is also supported by a Marie Sklodowska-Curie Actions Individual Fellowship (MSCA-IF) within the European Program Horizon 2020 (DRYFUN Project 656035). P.L. received support from the European Union's Seventh Framework Programme for research, technological development and demonstration under grant agreement no GA-2010-267243 – PLANT FELLOWS. N.G. has received the support of the EU in the framework of the Marie-Curie FP7 COFUND People Programme, through the award of an AgreenSkills + fellowship (under grant agreement n° 609398). C.R.F. is supported by a fellowship from the Conselho Nacional de Desenvolvimento Científico e Tecnológico - Brazil (PQ 305304/2013-5). F.T.M. acknowledges support from the Salvador de Madariaga program of the Spanish Ministry of Education, Culture and Sports (PRX14/00225) and the Research Exchange Program of the Hawkesbury Institute for the Environment during the writing of this article. We also are grateful to Dr. I. J. Wright for fruitful discussions and comments on earlier versions, and to Dr. A. Siefert for providing plant trait data.

LITERATURE CITED

Bernard-Verdier, M., M. Navas, M. Vellend, C. Violle, A. Fayolle and E. Garnier. 2012. Community assembly along a soil depth gradient: contrasting patterns of plant trait

402 convergence and divergence in a Mediterranean rangeland. Journal of Ecology 100: 1422-
403 1433.
404 Brown, JH., TJ. Valone and CG. Curtin. 1997. Reorganization of an arid ecosystem in
405 response to recent climate change. Proceeding of the National Academy of Sciences of the
406 United States of America 94: 9729-9733.
407 Chesson, P. 2000. Mechanisms of maintenance of species diversity. Annual Review of
408 Ecology and Systematics 31: 343–366.
409 Delgado-Baquerizo, M., FT. Maestre, A. Gallardo, MA. Bowker, MD. Wallenstein, JL. Quero et
410 al. 2013. Decoupling of soil nutrient cycles as a function of aridity in global drylands. Nature
411 502: 672–676.
412 Dubuis, A., L. Rossier, J. Pottier, L. Pellissier, P. Vittoz, and A. Guisan. 2013. Predicting
413 current and future spatial community patterns of plant functional traits. Ecography 36:
414 1158-1168.
415 Eldridge, DJ. 1999. Distribution and floristics of moss- and lichen-dominated soil crusts in a
416 patterned Callitris glaucophylla woodland in eastern Australia. Acta Oecologica 20: 159-
417 170.
418 Enquist, BJ. 2002. Universal scaling in tree and vascular plant allometry: toward a general
419 quantitative theory linking plant form and function from cell to ecosystem. Tree
420 Physiologist 22: 1045-1064.
421 Enquist, BJ., J. Norrberg, SP. Bonser, C. Violle, CT. Webb, A. Henderson et al. 2015. Scaling
422 from traits to ecosystems: developing a General Trait Theory via integrating Trait-based
423 and Metabolic Scaling theories. Advances in Ecological Research, in press.
424 Food and Agriculture Organization (FAO), World Reference Base for Soil Resources (FAO,
425 Rome, 1998).

Fonseca, CR., JM. Overton, B. Collins, and M. Westoby. 2000. Shifts in trait-combinations along rainfall and phosphorus gradients. Journal of Ecology 88: 964–977.

Frenette-Dussault, C., B. Shipley, JF Léger, D. Meziane and Y. Hingrat. 2012. Functional structure of an arid steppe plant community reveals similarities with Grime's C-S-R theory. Journal of Vegetation Science 23: 208–222.

Frenette-Dussault, C. B. Shipley, D. Meziane and Y. Hingrat. 2013. Trait-based climate change predictions of plant community structure in arid steppes. Journal of Ecology 101: 484-492.

Freschet, GT., AT. Dias, DD. Ackerly, R. Aerts, PM. van Bodegom, WK. Cornwell et al. 2011. Global to community scale differences in the prevalence of convergent over divergent leaf trait distributions in plant assemblages. Global Ecology and Biogeography 20: 755-765.

Fridley, JD., JP. Grime, AP. Askew, B. Moser and CJ. Stevens. 2011. Soil heterogeneity buffers community response to climate change in species-rich grassland. Global Change Biogeography 17: 2002-2011.

Gómez-Plaza, A., M. Martínez-Mena, J. Albaladejo and VM. Castillo. 2001. Factors regulating spatial distribution of soil water content in small semiarid catchments. Journal of Hydrology 253: 211–226.

Gross, N., TM. Robson, S. Lavorel, C. Albert, Y. Le Bagousse-Pinguet, and R. Guillemin. 2008. Plant response traits mediate the effects of subalpine grasslands on soil moisture. New Phytologist 180: 652-662.

Gross, N., L. Börger, SI. Soriano-Morales, Y. Le Bagousse-Pinguet, JL. Quero, M. García-Gómez et al. 2013. Uncovering multiscale effects of aridity and biotic interactions on the functional structure of Mediterranean shrublands. Journal of Ecology 101: 637-649.

Guo, Q., H. Zhongmin, L. Shenggong, L. Xuanran, S. Xiaomin and Y. Guirui. 2012. Spatial variations in aboveground net primary productivity along a climate gradient in Eurasian

temperate grassland: effects of mean annual precipitation and its seasonal distribution. Global Change Biology 18: 3624-3631.

Hijmans, R.J., SE. Cameron, JL. Parra, PG. Jones and A. Jarvis. 2005. Very high resolution interpolated climate surfaces for global land areas. International Journal of Climatology 25: 1965–1978.

IPCC 2013. Climate change 2013: the physical science basis. In: Contribution of Working Group I to the Fifth Assessment Report of the Intergovernmental Panel on Climate Change (eds Stocker TF, Qin D, Plattner G-K, Tignor M, Allen SK, Boschung J, Nauels A, Xia Y, Bex V, Midgley PM). Cambridge University Press, Cambridge, UK

Kattge, J., S. Diaz, S. Lavorel, IC. Prentice, P. Leadley, G. Bonisch et al. 2011. TRY – a global database of plant traits. Global Change Biology 17: 2905–2935.

Keddy, P. 1992. Assembly and response rules: two goals for predictive community ecology. Journal of Vegetation Science 3: 157–164.

Kraft, NJB., R. Valencia and DD. Ackerly. 2008. Functional traits and niche-based tree community assembly in an Amazonian forest. Science 322: 580–582.

Liancourt, P. LA. Spence, DS. Song, A. Lkhagva, A. Sharkuu, B. Boldgiv et al. 2013. Plant response to climate change varies with topography, interactions with neighbors, and ecotype. Ecology 94: 444-453.

Laughlin, DC., PZ. Fule, DW. Huffman, J. Crouse and E. Laliberté. 2011. Climatic controls on trait-based forest assembly. Journal of Ecology 99: 1489–1499.

Laughlin, DC., C. Joshi, SJ. Richardson, DA. Peltzer, NWM Mason and DA. Wardle. 2015. Quantifying multimodal trait distributions improves trait-based predictions of species abundances and functional diversity. Journal of Vegetation Science 26: 46-57.

Maestre, FT., R. Salguero-Gomez and JL. Quero. 2012a. It is getting hotter in here: determining and projecting the impacts of global environmental change on drylands. Philosophical Transactions of the Royal Society B 367: 3062-3075.

Maestre, FT., JL. Quero, NJ. Gotelli, A. Escudero, V. Ochoa, M. Delgado-Baquerizo et al. 2012b. Plant species richness and ecosystem multifunctionality in global drylands. Science 335: 214-218.

Moles, AT., SE. Perkins, SW. Laffan, H. Flores-Moreno, M. Awasthy, ML. Tindall et al. 2014. Which is a better predictor of plant traits: temperature or precipitation? Journal of Vegetation Science 25: 1167-1180.

Noy Meier, I. 1973. Desert ecosystems: environment and producers. Annual Review of Ecology and Systematics 4: 25-51.

Ordonez, JC., PM. van Bodegom, J-PM. Witte, IJ. Wright, PB. Reich and R. Aerts. 2009. A global study of relationships between leaf traits, climate and soil measures of nutrient fertility. Global Ecology and Biogeography 18: 137–149.

Pakeman, R. and HM. Quested. 2007. Sampling plant functional traits: what proportion of the species needs to be measured? Applied Vegetation Science 10: 91-96.

Parmesan, C., MT. Burrows, CM. Duarte, ES. Poloczanska, AJ. Richardson, DS. Schoeman et al. 2013. Beyond climate change attribution in conservation and ecological research. Ecology Letters 16: 58-71.

Peñuelas, J., J. Sardans, M. Estiarte, R. Ogaya, J. Carnicer, M. Coll et al. 2013. Evidence of current impact of climate change on life: a walk from genes to the biosphere. Global Change Biology 19: 2303–2338.

Reich, PB., IJ. Wright and CH. Lusk. 2007. Predicting leaf functional traits from simple plant and climate attributes using the GLOPNET global dataset. Ecological Applications 17: 1982–1988.

499 Safirel, U. and Z. Adeel Z 2005. Dryland systems. In: Hassan R, Scholes R, Neville A (eds)
500 Ecosystems and human well-being: current state and trends, vol 1. Island Press,
501 Washington, DC, pp 623–662
502 Schamp, BS., J. Chau and LW. Aarssen. 2008. Dispersion of traits related to competitive
503 ability in an old-field plant community. Journal of Ecology 96: 204–212.
504 Soudzilovskaia, N., TG. Elumeeva, VG. Onipchenko, II. Shidakov, FS. Salpagarova, AB.
505 Khubiev et al. 2013. Functional traits predict relationship between plant abundance
506 dynamic and long-term climate warming. Proceeding of the National Academy of Sciences
507 of the United States of America 110: 18180-18184.
508 Swenson, NG. and MD. Weiser. 2010. Plant geography upon the basis of functional traits: an
509 example from eastern North American trees. Ecology 91: 2234–2241.
510 Swenson, NG., BJ. Enquist, J. Pither, AJ. Kerkhoff, B. Boyle, MD. Weiser et al. 2012. The
511 biogeography and filtering of woody plant functional diversity in North and South America.
512 Global Ecology and Biogeography 21: 798-808.
513 Valencia, E., FT. Maestre, Y. Le Bagousse-Pinguet, JL. Quéro R. Tamme, L Börger et al.
514 2015. Functional diversity enhances the resistance of ecosystem multifunctionality to
515 aridity in Mediterranean drylands. New Phytologist, in press.
516 Violle, C., ML. Navas, D. Vile, E. Kazakou, C. Fortunel, I. Hummel et al. 2007. Let the
517 concept of trait be functional! Oikos 116: 882–892.
518 Violle, C., PB. Reich, SW. Pacala, BJ. Enquist and J. Kattge. 2014. The emergence and
519 promise of functional biogeography. Proceeding of the National Academy of Sciences of
520 the United States of America, doi/10.1073/pnas.1415442111
521 Walker MD et al. 2006. Plant community responses to experimental warming across the
522 tundra biome. Proceeding of the National Academy of Sciences of the United States of
523 America 103: 1342–1346.

524 Westoby, M. 1998. A leaf-height-seed (LHS) plant ecology strategy scheme. Plant and Soil
525 199: 213–227.
526 Wright, IJ., PB. Reich, M. Westoby, DD. Ackerly, Z. Baruch, F. Bongers, F. et al. 2004. The
527 worldwide leaf economics spectrum. Nature 428: 821–827.
528

529 **TABLE**

530 **TABLE 1.** Best-fitting regression models with and without interactions among predictors. Models are presented for each moment and each trait
531 separately. The best models are selected according to AICc values (Appendix S5). Shaded cells indicate variables that were selected in a
532 particular model. Latitude and longitude were introduced to avoid spatial auto-correlations. Slope directions are indicated when significant.
533 LL: latitude / longitude, MAT: mean temperature, MAP: mean precipitation, PS: precipitation seasonality, SL: slope, and SC: sand content
534

535 / 536 / 537 / 538 / 539

Trait	Interaction	Moment	LL	MAT	MAP	PS	SL	SD	MAT×MAP	MAT×PS	MAT×SL	MAT×SC	MAP×PS	MAP×SL	MAP×SC	PS×SL	PS×SC	SL×SC	Adj. R^2	AICc
SLA	Without interaction	Mean		-	+			-											0.396	179.42
		Var		-	+	-													0.247	413.32
		Skew			-														0.166	-62.74
		Kurt		+				-											0.092	439.13
	With interactions	Mean		+	+	+	-	+		-			-		-				0.594	137.05
		Var		+	+	+			-	-									0.410	388.06
		Skew		-	-	-		-		+			+				+		0.268	-68.01
		Kurt				+					+					-			0.165	432.12
Height	Without interaction	Mean		+		-	+												0.719	169.84
		Var				-													0.587	490.82
		Skew			+														0.113	-285.13
		Kurt		+	+														0.278	416.26
	With interactions	Mean							+	-	-	+			-	+			0.826	121.21
		Var			+			+	+		-		-		-	+			0.640	483.16
		Skew		-	+		+	+	+	+				-	-				0.295	-300.17
		Kurt		-		-	+		+	+				-	-				0.335	415.97

PeerJ Preprints | https://doi.org/10.7287/peerj.preprints.1913v1 | CC-BY 4.0 Open Access | rec: 31 Mar 2016, publ: 31 Mar 2016

FIGURE LEGENDS

FIG. 1. Formulas (after Enquist et al. 2015), shapes and ecological implications of the four moments of community trait distributions.

FIG. 2. Percentage of variance explained for each group of predictors (i.e. climate and topo-edaphic variables) and two-way interactions (a, b), and for each group of predictors and their interactions separately (c, d). Grey portions represent the unexplained variances. The proportions were calculated using a variance decomposition analysis based on the best model selected for each trait and moment (Table 1, Appendices S4 and S6).

FIG. 3. Predicted values (black dots) and planes representing the interactions between mean temperature (MAT) and precipitation seasonality, and between mean precipitation (MAP) and precipitation seasonality on the mean (a, b), variance (c, d) and skewness (e, f) for specific leaf area (SLA). The interactions were selected by the best fitting models (Table 1, Appendices S4 and S6). Effects of interactions are presented at low ($CV_{seasonality}$ = 12: a, c and e) and high seasonality ($CV_{seasonality}$ = 124: b,d and f). The colours of the predicted planes change from blue (low values of the moments) to red (high values).

FIG. 4. Predicted values (black dots) and planes representing the interactions between mean temperature (MAT) and sand content and between mean precipitation (MAP) and sand content on the mean (a, b), variance (c, d), skewness (e, f) and kurtosis (g, h) for height. The interactions were selected by the best fitting models (Table 1, Appendices S4 and S6). Effects of interactions are presented at low (sand content = 27.66%: a, c, e and g) and high sand content (sand content = 94.54%: b,d, f and h). The colours of the predicted planes change from blue (low values of the moments) to red (high values of the moments).

FIGURES

FIG. 1.

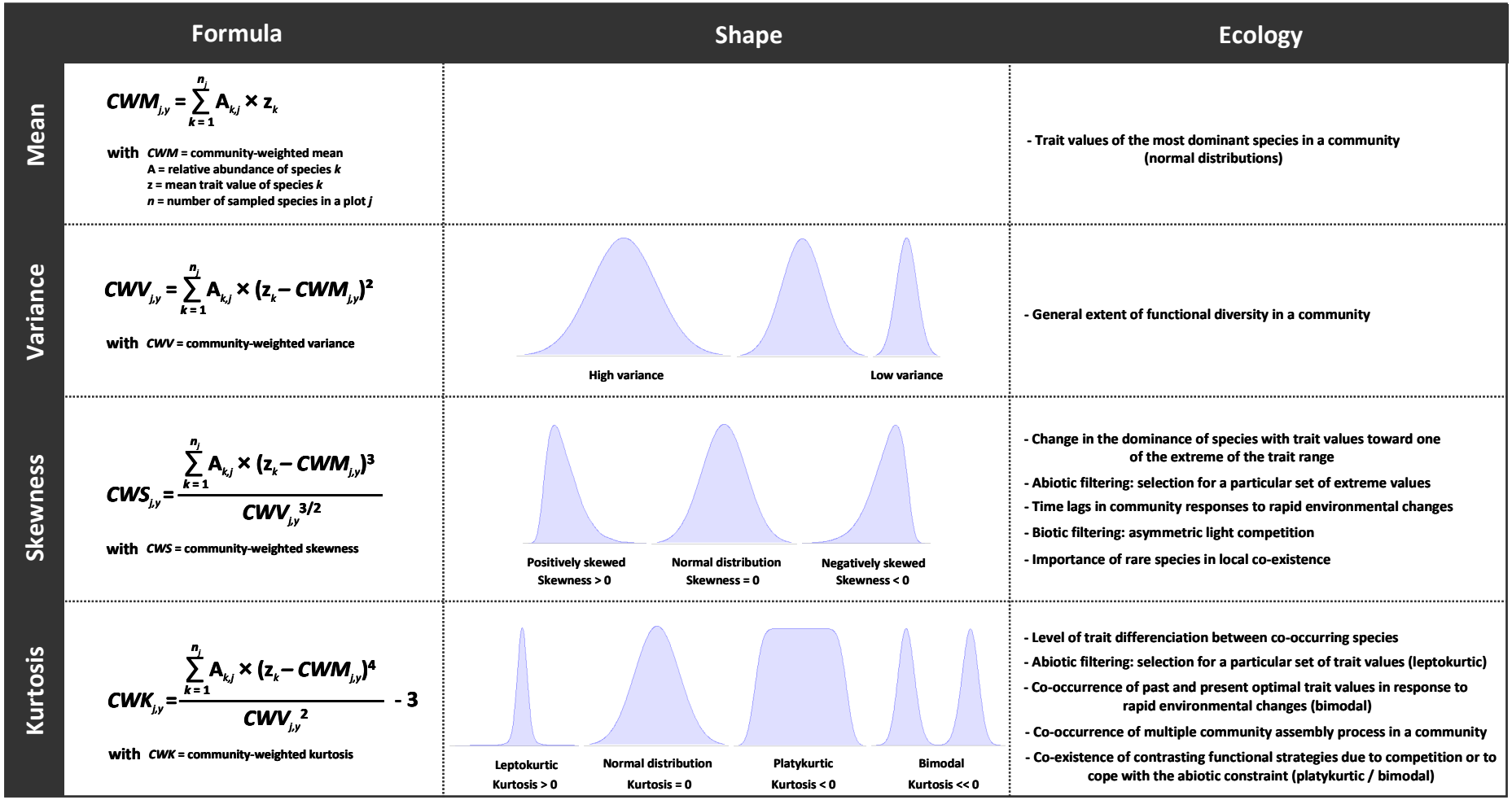

PeerJ Preprints | https://doi.org/10.7287/peerj.preprints.1913v1 | CC-BY 4.0 Open Access | rec: 31 Mar 2016, publ: 31 Mar 2016

FIG. 2.

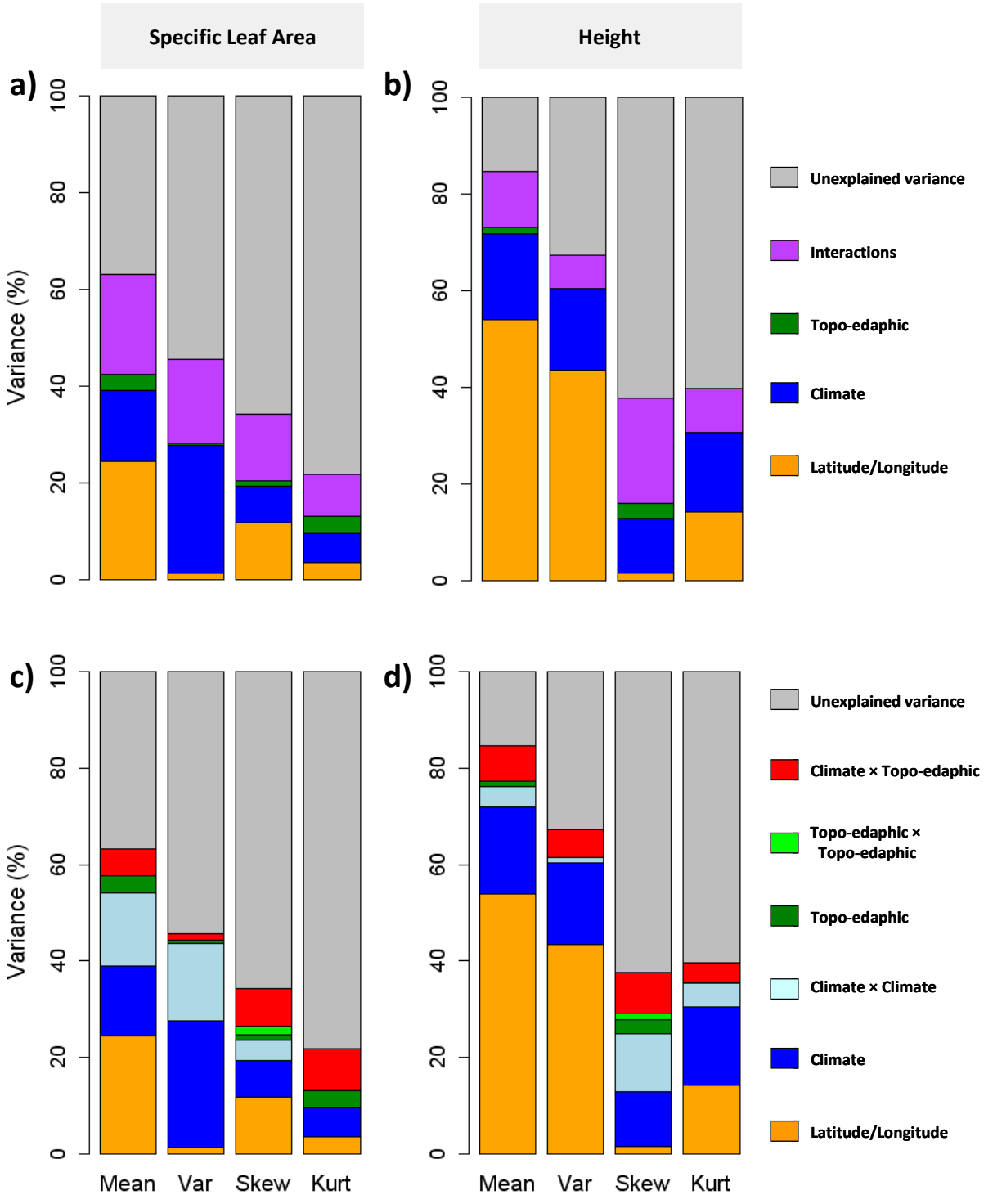

FIG. 3.

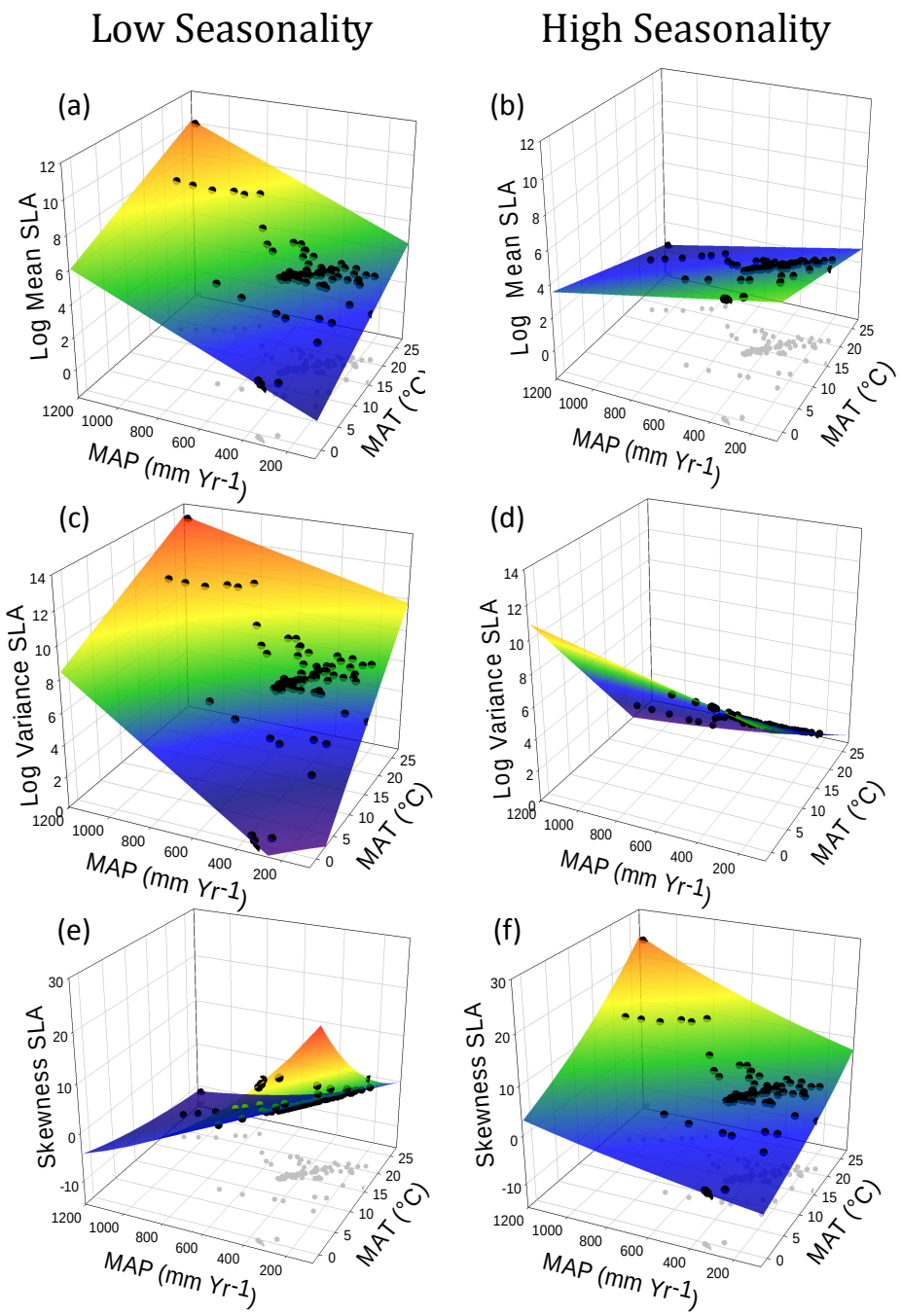

FIG. 4.

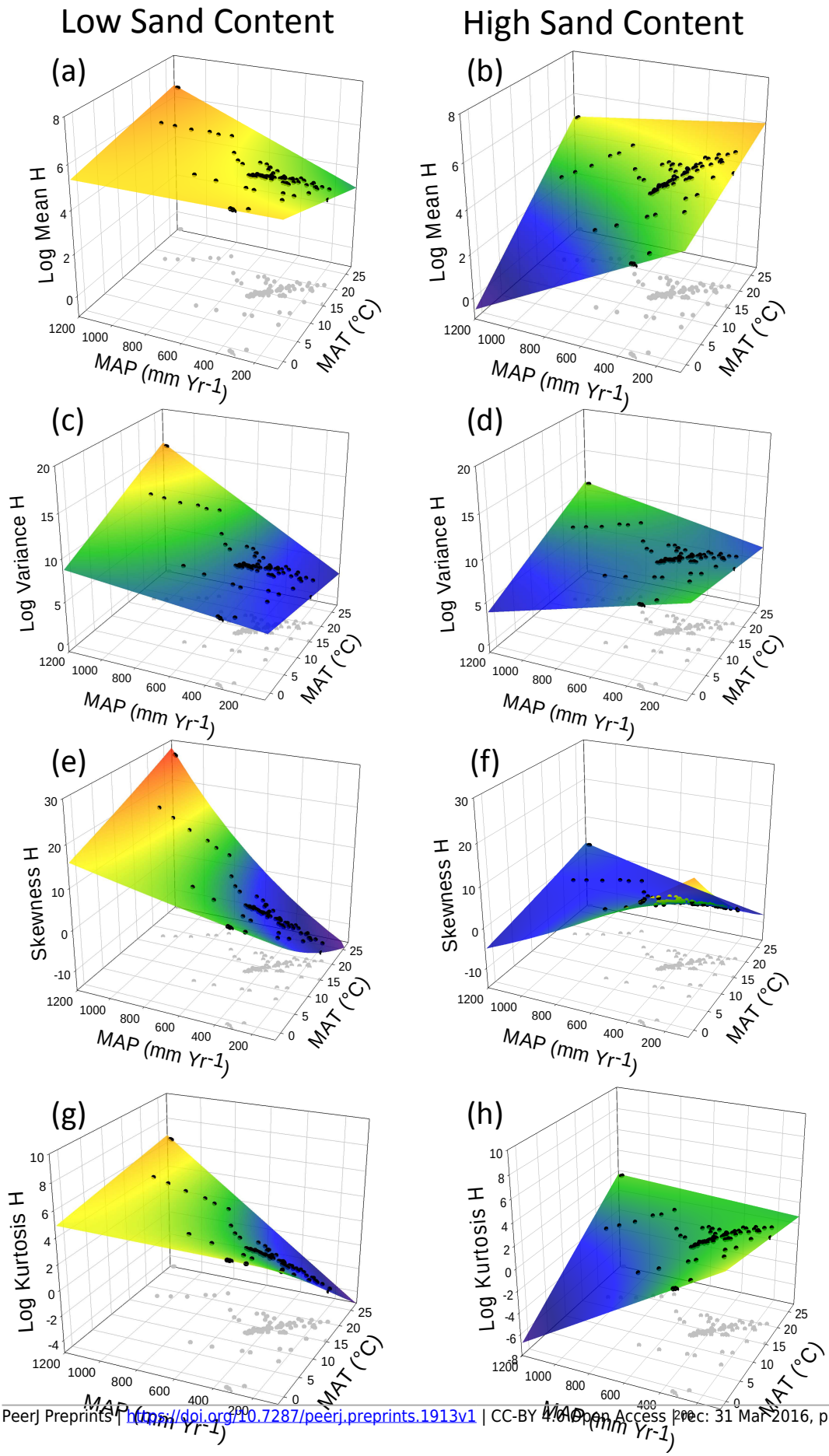

APPENDICES

APPENDIX S1. Map showing the sampling effort for a) the 130 studied dryland communities and b) the Mediterranean basin.

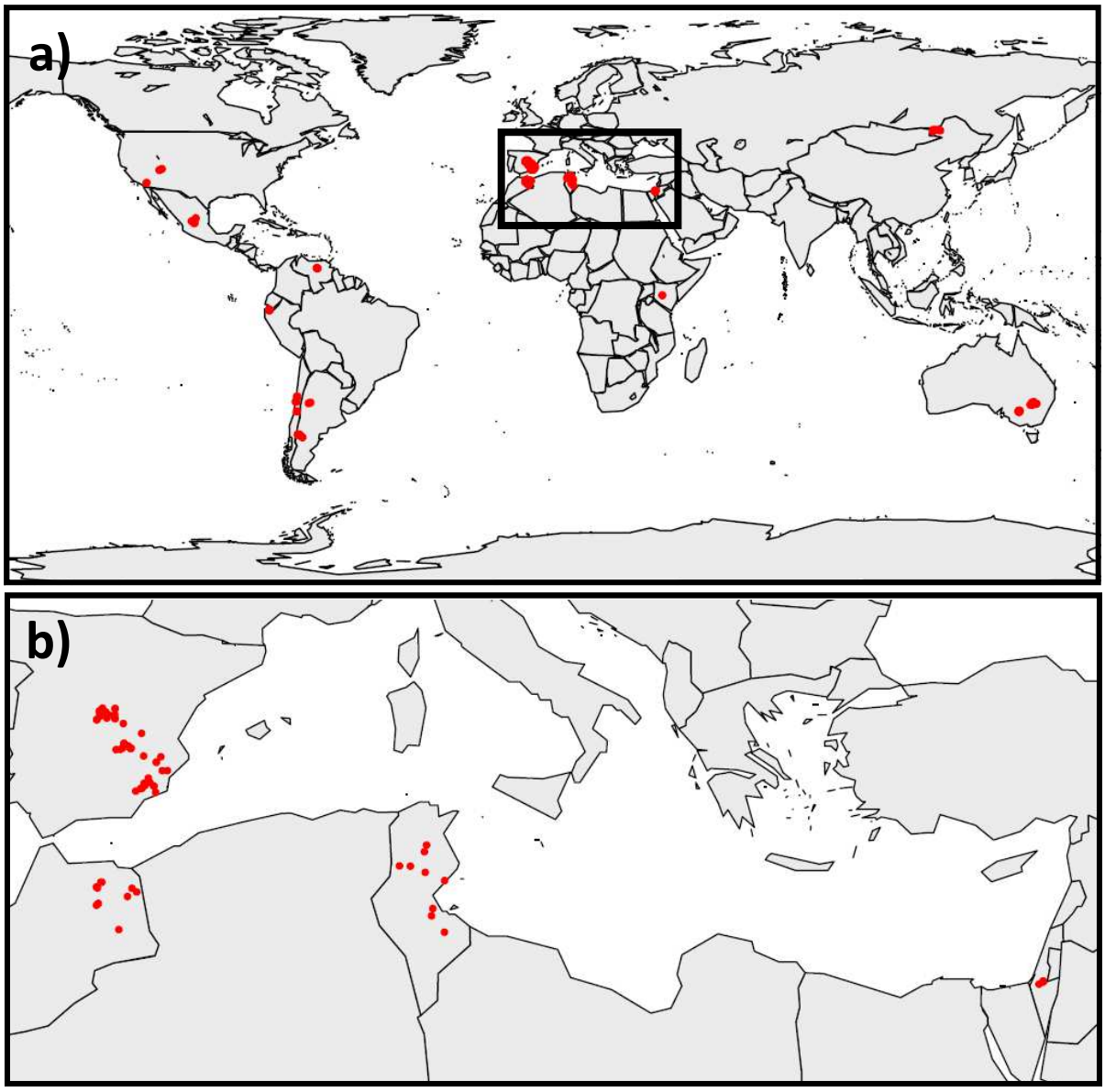

APPENDIX S2. Correlation matrices among the four moments (mean, variance, skewness and kurtosis) and among environmental predictors (climate and edaphic conditions). Correlations with Pearson coefficients higher than 0.50 (absolute value) are indicated in bold. We also present the results of the variance inflation factor (VIF) to evaluate the risk of multicollinearity.

Mean SLA	1.00							
Mean H	-0.11	1.00						
Var SLA	**0.58**	0.14	1.00					
Var H	-0.01	**0.84**	0.22	1.00				
Skew SLA	**-0.66**	0.05	**-0.51**	-0.10	1.00			
Skew H	0.23	-0.10	0.06	0.27	-0.27	1.00		
Kurt SLA	-0.37	0.10	**-0.66**	-0.07	**0.50**	-0.15	1.00	
Kurt H	-0.03	-0.27	-0.29	-0.29	0.07	0.37	0.29	1.00
	Mean SLA	**Mean H**	**Var SLA**	**Var H**	**Skew SLA**	**Skew H**	**Kurt SLA**	**Kurt H**

Latitude	1.00						
Longitude	-0.18	1.00					
MAT	-0.20	-0.05	1.00				
MAP	-0.06	-0.29	0.35	1.00			
Prec. season	-0.05	-0.36	-0.02	0.06	1.00		
Slope	0.33	-0.21	-0.08	0.18	-0.01	1.00	
Sand	-0.33	0.01	-0.02	-0.20	0.14	-0.39	1.00
	Latitude	**Longitude**	**MAT**	**MAP**	**Prec. season**	**Slope**	**Sand**

Model	Model r^2	VIF
MAT ~ MAP + Prec.season + Slope + sand	0.135	1.156
MAP ~ MAT + Prec.season + Slope + sand	0.173	1.209
Prec.season ~ MAT + MAP + Slope + sand	0.039	1.040
Slope ~ MAT + MAP + Prec.season + sand	0.194	1.241
Sand ~ MAT + MAP + Prec.season + Slope	0.195	1.242
Lat ~ MAT + MAP + prec.season + slope + sand	0.283	1.395
MAT ~ Lat + MAP + Prec.season + Slope + sand	0.158	1.187
MAP ~ Lat + MAT + Prec.season + Slope + sand	0.184	1.225
Prec.season ~ Lat + MAT + MAP + Slope + sand	0.040	1.041
Slope ~ Lat + MAT + MAP + Prec.season + sand	0.235	1.308
Sand ~ Lat + MAT + MAP + Prec.season + Slope	0.305	1.439
Long ~ MAT + MAP + prec.season + slope + sand	0.282	1.394
MAT ~ Long + MAP + Prec.season + Slope + sand	0.140	1.162
MAP ~ Long + MAT + Prec.season + Slope + sand	0.213	1.270
Prec.season ~ Long + MAT + MAP + Slope + sand	0.198	1.248
Slope ~ Long + MAT + MAP + Prec.season + sand	0.201	1.252
Sand ~ Long + MAT + MAP + Prec.season + Slope	0.245	1.324

APPENDIX S3. Species number (Sp.nb) and abundance of perennial vegetation for which trait data were available in each of the 130 sites**.** Data are shown for both Specific Leaf Area and maximum plant height.

			Specific Leaf Area (SLA)		Maximum plant height	
Country	**Latitude (°)**	**Longitude (°)**	**Sp. nb**	**% abundance**	**Sp. nb**	**% abundance**
Argentina	-41.81	-69.68	7	92.94	13	99.95
Argentina	-41.24	-70.42	9	91.52	19	99.80
Argentina	-41.11	-70.89	10	86.89	20	98.17
Argentina	-41.00	-71.06	9	98.98	13	100.00
Argentina	-41.03	-70.52	7	77.18	19	100.00
Argentina	-31.49	-67.28	5	76.59	4	64.54
Argentina	-31.72	-67.84	5	98.67	2	74.76
Australia	-34.22	142.55	12	99.12	15	100.00
Australia	-34.20	142.56	16	97.93	21	100.00
Australia	-34.25	142.48	16	99.27	16	100.00
Australia	-34.02	142.51	12	98.17	13	100.00
Australia	-34.11	142.54	12	82.58	15	100.00
Australia	-34.20	142.42	12	98.41	15	100.00
Australia	-33.96	142.46	10	98.44	12	100.00
Australia	-33.97	142.66	11	91.90	14	100.00
Australia	-34.11	142.57	15	95.16	16	100.00
Australia	-33.96	142.46	11	99.29	14	100.00
Australia	-33.93	142.69	13	99.78	17	100.00
Australia	-33.94	142.67	15	99.73	18	100.00
Australia	-32.16	145.89	20	91.69	27	99.59
Australia	-31.56	146.31	31	94.71	38	99.79
Australia	-31.30	146.91	16	96.77	24	99.86
Australia	-31.86	147.71	27	84.46	39	99.92
Australia	-32.12	146.66	17	84.00	19	100.00
Chile	-34.11	-71.35	3	86.23	4	95.46
Chile	-29.75	-71.25	4	76.69	8	95.01
Chile	-29.75	-71.25	5	77.13	14	86.28
Chile	-29.75	-71.25	5	70.81	11	83.54
Chile	-31.20	-71.58	3	71.08	11	98.72
Chile	-31.20	-71.58	3	78.43	10	96.26
Chile	-31.20	-71.59	3	76.95	9	90.99
China	49.26	119.18	11	88.03	9	85.87
China	49.49	118.40	14	62.00	9	84.60
China	49.53	117.27	11	95.39	7	94.50
China	49.03	116.99	10	81.44	5	68.05
Ecuador	-3.98	-79.43	3	63.48	3	67.62
Ecuador	-4.00	-79.43	3	71.09	5	71.50
Ecuador	-4.00	-79.44	3	63.40	3	67.54
Ecuador	-4.00	-79.50	3	71.65	5	72.62
Ecuador	-4.00	-79.49	4	76.66	5	78.45
Ecuador	-4.00	-79.50	4	61.14	6	61.26
Ecuador	-4.01	-79.49	4	88.31	5	89.71
Ecuador	-4.01	-79.49	4	66.27	4	66.27
Israel	31.36	34.82	5	100.00	5	100.00
Israel	31.36	34.82	6	100.00	6	100.00

Israel	31.36	34.82	6	100.00	6	100.00
Israel	31.36	34.82	5	100.00	5	100.00
Israel	31.36	34.82	6	100.00	6	100.00
Israel	31.36	34.82	6	100.00	6	100.00
Israel	31.27	34.65	3	97.10	4	100.00
Kenya	0.35	36.89	9	69.02	17	78.35
Mexico	23.21	-101.27	6	76.03	7	80.84
Mexico	22.35	-102.46	3	78.13	3	78.37
Mexico	21.77	-101.67	3	74.21	4	98.49
Mexico	21.77	-101.67	3	74.88	4	76.67
Morocco	34.16	-2.37	7	92.75	8	93.44
Morocco	34.43	-2.19	8	99.68	6	99.46
Morocco	34.47	-3.64	6	99.22	6	100.00
Morocco	34.44	-3.59	6	97.01	7	98.08
Morocco	34.31	-2.00	7	85.55	8	85.55
Morocco	33.87	-3.63	7	98.89	7	99.81
Morocco	33.93	-3.56	3	91.09	2	91.94
Morocco	33.07	-2.73	4	72.36	5	82.62
Morocco	34.63	-3.41	5	80.76	4	72.36
Morocco	34.63	-3.46	5	80.69	5	80.76
Spain	39.05	-2.23	10	100.00	12	100.00
Spain	39.05	-2.23	7	98.36	9	98.47
Spain	40.33	-3.42	7	99.89	7	99.49
Spain	40.32	-3.43	9	99.76	9	99.38
Spain	40.25	-3.26	7	71.85	10	75.26
Spain	37.80	-1.30	20	94.22	23	94.42
Spain	37.80	-1.31	16	95.68	21	96.03
Spain	40.27	-3.51	10	72.52	14	88.98
Spain	40.27	-3.51	3	60.57	4	80.18
Spain	40.14	-3.13	4	76.08	5	83.15
Spain	40.07	-2.90	27	93.90	29	94.81
Spain	40.07	-2.90	20	96.34	21	95.51
Spain	40.21	-3.42	14	98.45	15	95.63
Spain	40.21	-3.42	12	98.70	13	99.60
Spain	39.99	-3.62	6	96.77	7	96.09
Spain	39.99	-3.62	3	95.87	5	96.83
Spain	39.99	-3.62	4	72.84	5	85.89
Spain	37.82	-1.67	18	98.52	17	98.74
Spain	37.82	-1.67	13	95.33	17	95.45
Spain	40.19	-3.50	11	99.22	12	98.93
Spain	40.04	-3.21	7	92.91	7	94.53
Spain	39.21	-2.51	10	97.31	9	99.34
Spain	39.21	-2.51	9	94.97	11	99.44
Spain	38.59	-1.20	26	93.64	31	98.97
Spain	38.59	-1.20	15	88.72	23	93.49
Spain	40.36	-2.88	24	99.69	27	99.53
Spain	40.36	-2.88	21	96.81	24	99.23
Spain	38.79	-1.72	15	100.00	15	100.00
Spain	38.31	-0.76	12	97.23	15	96.66
Spain	39.04	-2.26	8	99.94	8	99.94
Spain	39.01	-2.66	8	97.74	9	94.83
Spain	37.72	-1.84	10	99.65	12	98.62
Spain	40.16	-2.89	28	97.74	29	98.65
Spain	37.92	-1.47	8	97.28	10	98.37

Spain	37.73	-1.78	7	94.32	9	94.67
Spain	38.31	-0.96	17	98.80	17	99.10
Spain	40.37	-3.39	10	99.97	10	99.59
Spain	37.59	-1.23	6	98.79	8	99.47
Spain	39.54	-1.80	18	99.36	20	93.77
Spain	38.07	-1.53	13	99.44	12	97.65
Spain	39.13	-2.35	6	99.98	6	99.98
Spain	38.77	-1.02	7	95.45	9	96.71
Spain	39.00	-2.84	16	98.40	20	99.99
Spain	39.05	-2.57	7	97.85	11	98.16
Spain	40.02	-2.88	18	86.58	20	95.45
Spain	40.26	-3.49	9	100.00	11	99.51
Spain	37.63	-2.04	9	99.95	10	99.43
Spain	40.11	-3.46	12	99.90	15	99.47
Spain	39.86	-2.54	12	63.25	18	85.60
Spain	37.89	-1.70	14	84.85	18	84.12
Tunisia	35.17	8.67	7	96.80	7	97.05
Tunisia	33.52	9.97	6	88.72	7	97.36
Tunisia	35.16	9.12	6	96.79	6	97.03
Tunisia	34.96	9.72	4	100.00	4	100.00
Tunisia	32.98	10.50	4	86.08	5	95.19
Tunisia	34.69	10.51	8	81.32	10	82.27
Tunisia	33.76	10.03	8	86.83	9	78.96
Tunisia	35.63	9.69	5	74.35	7	82.26
Tunisia	35.86	9.77	6	95.39	6	71.89
USA	37.85	-111.31	6	76.10	7	81.89
USA	37.51	-112.02	6	86.90	7	98.10
USA	33.75	-115.81	3	78.20	3	83.80
Venezuela	8.43	-65.40	5	89.87	8	99.36
Venezuela	8.43	-65.41	5	95.16	10	100.00
Venezuela	8.32	-65.19	3	86.38	7	100.00
Mean			**9.4 ± (sd) 6.04**	**89.48 ± (sd) 11.29**	**11.45 ± (sd) 7.32**	**92.77 ± (sd) 9.89**

APPENDIX S4. Results of analyses using community abundances above 80% (n = 95 communities. a) Best-fitting regression models in absence of interactions among predictors. Models are presented for each moment and each trait separately. The best models are selected according to AICc values. Shaded cells indicate variables that were selected in a particular model. Latitude and longitude were introduced to avoid spatial auto-correlations. Slope directions are indicated when significant. b) Proportion of variance explained for each group of predictors (i.e. climate and topo-edaphic variables) and two-way interactions (a. and b). and for each group of predictors and their interactions separately (c and d). Grey portions represent the unexplained variances. The proportions were calculated using a variance decomposition analysis based on the best model selected for each trait and each moment.

LL: latitude and longitude. MAT: mean annual temperature. MAP: mean annual precipitation. PS: precipitation seasonality, SL: slope angle, SC: sand content.

Trait	Moment	LL	MAT	MAP	PS	SL	SC	Adj. R^2	AICc
SLA	Mean		-	+	-			0.306	128.48
	Var		-	+	-			0.391	285.39
	Skew		+	-	+			0.192	-88.45
	Kurt		+		+		-	0.182	311.40
Height	Mean			+	-			0.811	104.03
	Var			+	-			0.655	359.43
	Skew			+				0.222	-224.84
	Kurt			+				0.325	303.13

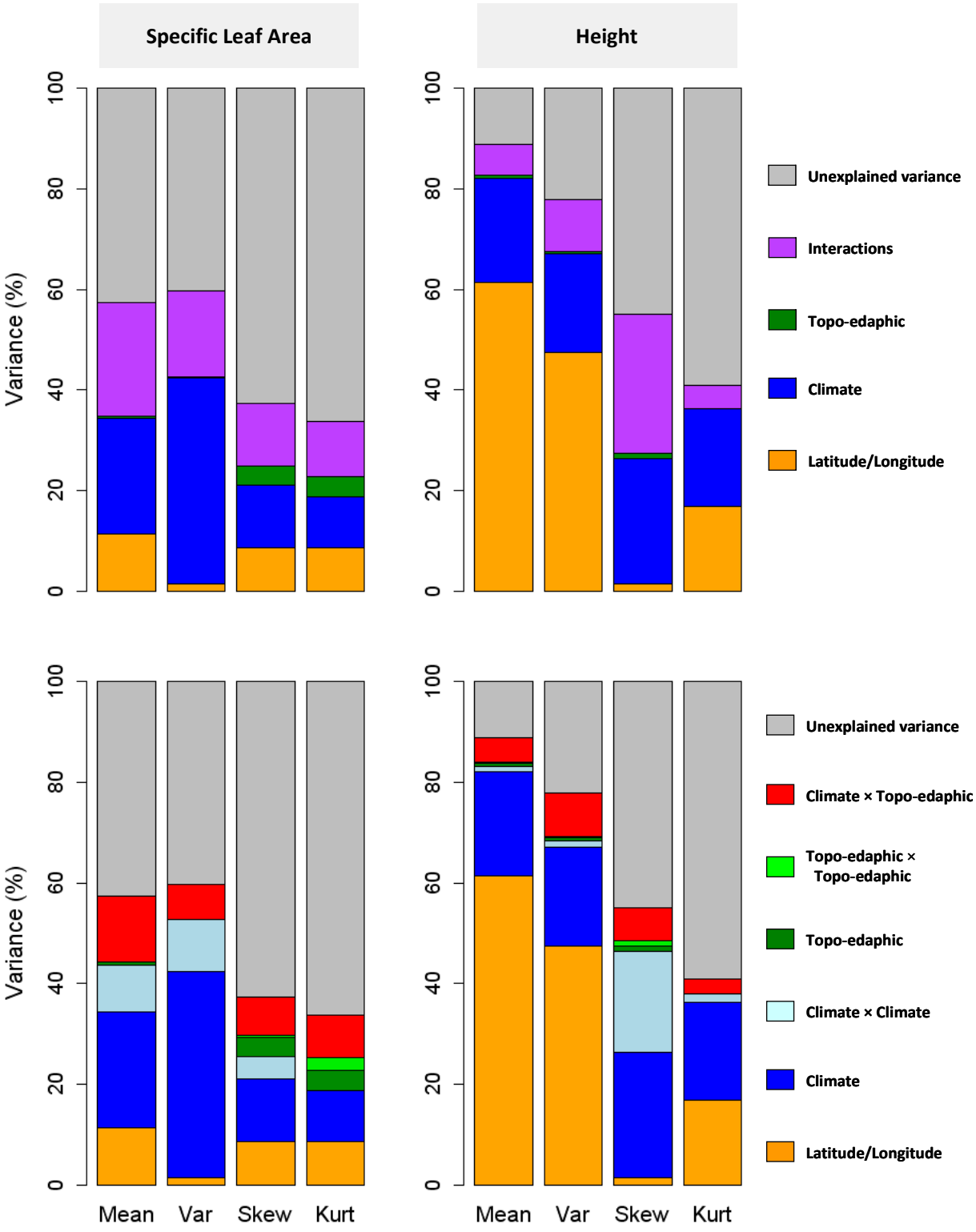
Specific Leaf Area
Height
Variance (%)
0
20
40
60
80
100
Mean
Var
Skew
Kurt
Unexplained variance
Interactions
Topo-edaphic
Climate
Latitude/Longitude
Climate × Topo-edaphic
Topo-edaphic × Topo-edaphic
Climate × Climate

APPENDIX S5. Boxplots representing the ranges of data for community-weighted mean, variance, skewness and kurtosis for both specific leaf area (SLA) and maximum plant height. The grey boxes represent the envelope of the 50% central region

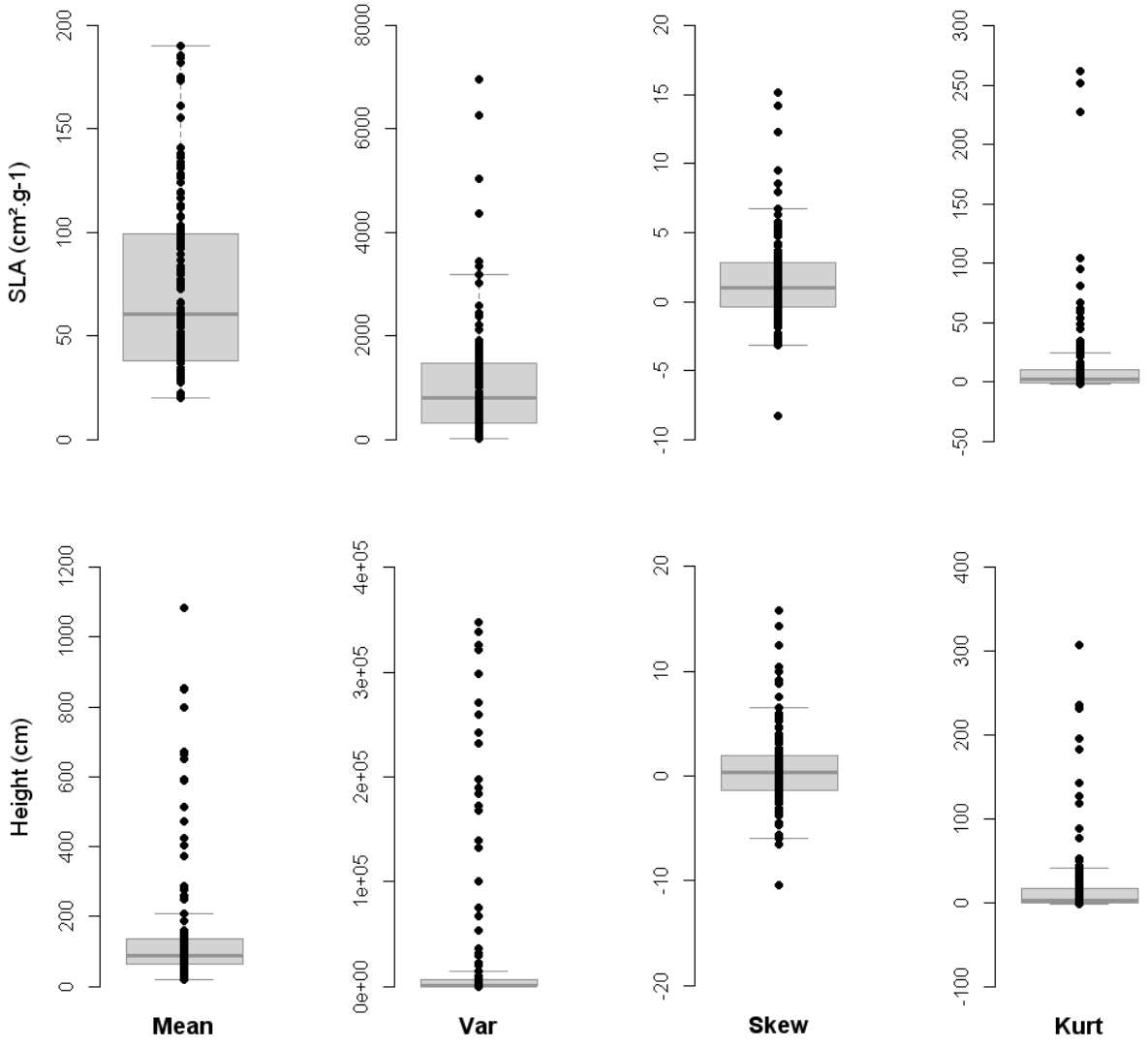

APPENDIX S6. Best models selected from the multiple regressions including geographical, climatic and edaphic variables as predictors (Table 1) and with interactions among predictors (Table 2). Models are presented for each moment separately for a) specific leaf area and b) height.

P values of each best multiple regression model are indicated as follows: ns = $P > 0.05$. * =. $P < 0.05$. ** = $P < 0.01$. *** = $P < 0.001$).

a) Specific Leaf Area (SLA)

Mean

```
Coefficients:
                   Estimate Std. Error t value Pr(>|t|)
(Intercept)         4.12110    0.04091 100.734  < 2e-16 ***
Latitude           -0.19960    0.04637  -4.305 3.36e-05 ***
Longitude          -0.29176    0.04420  -6.601 1.07e-09 ***
mean_temp          -0.23849    0.04434  -5.378 3.60e-07 ***
mean_precipitation  0.12558    0.04637   2.708  0.00772 **
sand               -0.11461    0.04542  -2.524  0.01288 *
---
Signif. codes:  0 ‘***’ 0.001 ‘**’ 0.01 ‘*’ 0.05 ‘.’ 0.1 ‘ ’ 1

Residual standard error: 0.4665 on 124 degrees of freedom
Multiple R-squared: 0.4197,    Adjusted R-squared: 0.3963
F-statistic: 17.94 on 5 and 124 DF,  p-value: 2.354e-13
```

Mean + interactions

```
Coefficients:
                             Estimate Std. Error t value Pr(>|t|)
(Intercept)                   4.10656    0.03550 115.665  < 2e-16 ***
Latitude                     -0.05148    0.05004  -1.029  0.30572
Longitude                    -0.51606    0.06409  -8.052 7.63e-13 ***
mean_temp                     0.22597    0.09042   2.499  0.01384 *
mean_precipitation            0.48790    0.08786   5.553 1.78e-07 ***
prec_season                  -0.28308    0.06637  -4.265 4.07e-05 ***
slope                        -0.04601    0.04333  -1.062  0.29052
sand                          0.00305    0.04905   0.062  0.95052
mean_temp:prec_season        -0.30009    0.05387  -5.570 1.65e-07 ***
mean_temp:slope               0.08965    0.07880   1.138  0.25753
mean_precipitation:prec_season -0.41290    0.09583  -4.309 3.44e-05 ***
mean_precipitation:sand      -0.10807    0.03072  -3.518  0.00062 ***
prec_season:slope             0.11759    0.06453   1.822  0.07098 .
---
Signif. codes:  0 ‘***’ 0.001 ‘**’ 0.01 ‘*’ 0.05 ‘.’ 0.1 ‘ ’ 1

Residual standard error: 0.3826 on 117 degrees of freedom
Multiple R-squared: 0.6317,    Adjusted R-squared: 0.594
F-statistic: 16.72 on 12 and 117 DF,  p-value: < 2.2e-16
```

Variance

```
Coefficients:
                   Estimate Std. Error t value Pr(>|t|)
(Intercept)          6.4252     0.1006  63.879  < 2e-16 ***
Latitude            -0.2657     0.1068  -2.488  0.01415 *
Longitude           -0.3195     0.1192  -2.681  0.00834 **
mean_temp           -0.5618     0.1101  -5.101 1.23e-06 ***
```


PeerJ Preprints | https://doi.org/10.7287/peerj.preprints.1913v1 | CC-BY 4.0 Open Access | rec: 31 Mar 2016, publ: 31 Mar 2016

```
mean_precipitation   0.3202     0.1111   2.883  0.00465 **
prec_season         -0.5362     0.1131  -4.743 5.70e-06 ***
---
Signif. codes:  0 ‘***’ 0.001 ‘**’ 0.01 ‘*’ 0.05 ‘.’ 0.1 ‘ ’ 1

Residual standard error: 1.147 on 124 degrees of freedom
Multiple R-squared: 0.2765.    Adjusted R-squared: 0.2473
F-statistic: 9.476 on 5 and 124 DF.  p-value: 1.131e-07
```

Variance + interactions

```
Coefficients:
                              Estimate Std. Error t value Pr(>|t|)
(Intercept)                    6.40009    0.09812  65.226  < 2e-16 ***
Latitude                      -0.16409    0.10793  -1.520 0.131083
Longitude                     -0.92322    0.15883  -5.813 5.26e-08 ***
mean_temp                      0.45439    0.20821   2.182 0.031049 *
mean_precipitation             0.72447    0.20473   3.539 0.000575 ***
prec_season                   -0.98249    0.15751  -6.238 7.03e-09 ***
slope                         -0.12570    0.11105  -1.132 0.259963
mean_temp:mean_precipitation  -0.18363    0.09010  -2.038 0.043760 *
mean_temp:prec_season         -0.77997    0.14247  -5.475 2.48e-07 ***
mean_precipitation:prec_season -0.34769    0.20356  -1.708 0.090235 .
mean_precipitation:slope       0.20269    0.12397   1.635 0.104700
---
Signif. codes:  0 ‘***’ 0.001 ‘**’ 0.01 ‘*’ 0.05 ‘.’ 0.1 ‘ ’ 1

Residual standard error: 1.015 on 119 degrees of freedom
Multiple R-squared: 0.4557.    Adjusted R-squared:  0.41
F-statistic: 9.964 on 10 and 119 DF.  p-value: 5.501e-12
```

Skewness

```
Coefficients:
                 Estimate Std. Error t value Pr(>|t|)
(Intercept)       2.78190    0.01619 171.799  < 2e-16 ***
Latitude          0.01688    0.01694   0.996  0.32096
Longitude         0.05538    0.01732   3.197  0.00176 **
mean_temp         0.02871    0.01753   1.638  0.10390
mean_precipitation -0.05958    0.01788  -3.333  0.00113 **
---
Signif. codes:  0 ‘***’ 0.001 ‘**’ 0.01 ‘*’ 0.05 ‘.’ 0.1 ‘ ’ 1

Residual standard error: 0.1846 on 125 degrees of freedom
Multiple R-squared: 0.1914.    Adjusted R-squared: 0.1655
F-statistic: 7.398 on 4 and 125 DF.  p-value: 2.217e-05
```

Skewness+ interactions

```
Coefficients:
                              Estimate Std. Error t value Pr(>|t|)
(Intercept)                   2.800172   0.018195 153.894  < 2e-16 ***
Latitude                     -0.020416   0.022741  -0.898  0.37116
Longitude                     0.130593   0.029579   4.415 2.28e-05 ***
mean_temp                    -0.064449   0.035615  -1.810  0.07295 .
mean_precipitation           -0.135138   0.041304  -3.272  0.00141 **
prec_season                   0.061300   0.028120   2.180  0.03128 *
slope                         0.034268   0.020595   1.664  0.09884 .
sand                          0.007016   0.022150   0.317  0.75199
mean_temp:prec_season         0.079503   0.025505   3.117  0.00230 **
mean_precipitation:prec_season  0.104395   0.047522   2.197  0.03002 *
mean_precipitation:slope     -0.033637   0.022842  -1.473  0.14357
prec_season:slope            -0.036113   0.032406  -1.114  0.26742
prec_season:sand              0.048707   0.023901   2.038  0.04384 *
slope:sand                    0.043777   0.025423   1.722  0.08774 .
---
Signif. codes:  0 ‘***’ 0.001 ‘**’ 0.01 ‘*’ 0.05 ‘.’ 0.1 ‘ ’ 1
```

```
Residual standard error: 0.1729 on 116 degrees of freedom
Multiple R-squared: 0.342.    Adjusted R-squared: 0.2683
F-statistic: 4.639 on 13 and 116 DF.  p-value: 2.21e-06
```

Kurtosis

```
Coefficients:
            Estimate Std. Error t value Pr(>|t|)
(Intercept)   1.8873     0.1111  16.991   <2e-16 ***
Latitude     -0.1645     0.1260  -1.305   0.1944
Longitude     0.2749     0.1271   2.163   0.0325 *
mean_temp     0.2854     0.1170   2.439   0.0161 *
prec_season   0.2260     0.1252   1.805   0.0736 .
sand         -0.2585     0.1205  -2.145   0.0339 *
---
Signif. codes:  0 ‘***’ 0.001 ‘**’ 0.01 ‘*’ 0.05 ‘.’ 0.1 ‘ ’ 1

Residual standard error: 1.266 on 124 degrees of freedom
Multiple R-squared: 0.1281.    Adjusted R-squared: 0.09293
F-statistic: 3.643 on 5 and 124 DF.  p-value: 0.004137
```

Kurtosis + interactions

```
Coefficients:
                  Estimate Std. Error t value Pr(>|t|)
(Intercept)        1.936173   0.107946  17.937  < 2e-16 ***
Latitude          -0.231775   0.137831  -1.682 0.095228 .
Longitude          0.521882   0.140738   3.708 0.000316 ***
mean_temp          0.622793   0.155102   4.015 0.000103 ***
prec_season        0.074760   0.127431   0.587 0.558520
slope             -0.003104   0.133272  -0.023 0.981459
sand              -0.231873   0.128036  -1.811 0.072622 .
mean_temp:slope    0.605646   0.223593   2.709 0.007734 **
prec_season:slope -0.623508   0.187514  -3.325 0.001170 **
---
Signif. codes:  0 ‘***’ 0.001 ‘**’ 0.01 ‘*’ 0.05 ‘.’ 0.1 ‘ ’ 1

Residual standard error: 1.215 on 121 degrees of freedom
Multiple R-squared: 0.2167.    Adjusted R-squared: 0.1649
F-statistic: 4.185 on 8 and 121 DF.  p-value: 0.0001894
```

B) Height

Mean

```
Coefficients:
            Estimate Std. Error t value Pr(>|t|)
(Intercept)  4.63717    0.03943 117.606  < 2e-16 ***
Latitude    -0.51669    0.04585 -11.268  < 2e-16 ***
Longitude    0.23301    0.04595   5.071 1.41e-06 ***
mean_temp    0.09862    0.04129   2.388   0.0184 *
prec_season -0.35912    0.04437  -8.094 4.54e-13 ***
slope        0.10326    0.04533   2.278   0.0244 *
---
Signif. codes:  0 ‘***’ 0.001 ‘**’ 0.01 ‘*’ 0.05 ‘.’ 0.1 ‘ ’ 1

Residual standard error: 0.4496 on 124 degrees of freedom
Multiple R-squared: 0.7297.    Adjusted R-squared: 0.7188
F-statistic: 66.94 on 5 and 124 DF.  p-value: < 2.2e-16
```

Mean + interactions

```
Coefficients:
                          Estimate Std. Error t value Pr(>|t|)
(Intercept)                4.52395    0.03533 128.042  < 2e-16 ***
Latitude                  -0.46556    0.04678  -9.953  < 2e-16 ***
Longitude                  0.12123    0.06113   1.983 0.049744 *
```

```
mean_temp                    0.11990    0.08069   1.486 0.140049
mean_precipitation          -0.05866    0.05720  -1.026 0.307249
prec_season                 -0.40401    0.04603  -8.778 1.92e-14 ***
slope                        0.13235    0.04079   3.245 0.001541 **
sand                        -0.04307    0.04579  -0.941 0.348932
mean_temp:mean_precipitation 0.10172    0.03920   2.595 0.010701 *
mean_temp:prec_season       -0.12637    0.05207  -2.427 0.016792 *
mean_temp:slope             -0.14775    0.07355  -2.009 0.046907 *
mean_temp:sand               0.13374    0.04297   3.112 0.002348 **
mean_precipitation:slope     0.10158    0.06357   1.598 0.112810
mean_precipitation:sand     -0.18136    0.05183  -3.499 0.000666 ***
prec_season:slope            0.17422    0.06172   2.823 0.005619 **
prec_season:sand             0.06777    0.04678   1.449 0.150197
---
Signif. codes:  0 ‘***’ 0.001 ‘**’ 0.01 ‘*’ 0.05 ‘.’ 0.1 ‘ ’ 1

Residual standard error: 0.3539 on 114 degrees of freedom
Multiple R-squared: 0.846,    Adjusted R-squared: 0.8258
F-statistic: 41.76 on 15 and 114 DF,  p-value: < 2.2e-16
```

Variance

```
Coefficients:
            Estimate Std. Error t value Pr(>|t|)
(Intercept)   7.5762     0.1361  55.652  < 2e-16 ***
Latitude     -1.0569     0.1444  -7.320 2.65e-11 ***
Longitude     0.6818     0.1557   4.380 2.48e-05 ***
mean_temp     0.2267     0.1426   1.590    0.114
prec_season  -1.0158     0.1530  -6.641 8.56e-10 ***
---
Signif. codes:  0 ‘***’ 0.001 ‘**’ 0.01 ‘*’ 0.05 ‘.’ 0.1 ‘ ’ 1

Residual standard error: 1.552 on 125 degrees of freedom
Multiple R-squared: 0.5994,    Adjusted R-squared: 0.5866
F-statistic: 46.76 on 4 and 125 DF,  p-value: < 2.2e-16
```

Variance + interactions

```
Coefficients:
                             Estimate Std. Error t value Pr(>|t|)
(Intercept)                   7.43040    0.14409  51.569  < 2e-16 ***
Latitude                     -0.83856    0.18904  -4.436 2.09e-05 ***
Longitude                     0.50633    0.17755   2.852  0.00514 **
mean_temp                    -0.01185    0.19932  -0.059  0.95268
mean_precipitation            0.75901    0.35186   2.157  0.03304 *
prec_season                  -1.30106    0.21038  -6.184 9.43e-09 ***
slope                         0.10508    0.16356   0.642  0.52185
sand                          0.18770    0.19131   0.981  0.32854
mean_temp:mean_precipitation  0.29248    0.14754   1.982  0.04978 *
mean_temp:slope              -0.61931    0.29276  -2.115  0.03651 *
mean_precipitation:prec_season -0.94856    0.34511  -2.749  0.00694 **
mean_precipitation:sand      -0.31961    0.12407  -2.576  0.01124 *
prec_season:slope             0.72310    0.24419   2.961  0.00371 **
---
Signif. codes:  0 ‘***’ 0.001 ‘**’ 0.01 ‘*’ 0.05 ‘.’ 0.1 ‘ ’ 1

Residual standard error: 1.448 on 117 degrees of freedom
Multiple R-squared: 0.6736,    Adjusted R-squared: 0.6401
F-statistic: 20.12 on 12 and 117 DF,  p-value: < 2.2e-16
```

Skewness

```
Coefficients:
                   Estimate Std. Error t value Pr(>|t|)
(Intercept)       3.8123088  0.0068842 553.777  < 2e-16 ***
Latitude          0.0060895  0.0076358   0.797   0.4267
Longitude         0.0004769  0.0074329   0.064   0.9489
mean_precipitation 0.0317211  0.0074923   4.234 4.41e-05 ***
```

```
sand                0.0131745  0.0076314   1.726   0.0868 .
---
Signif. codes:  0 ‘***’ 0.001 ‘**’ 0.01 ‘*’ 0.05 ‘.’ 0.1 ‘ ’ 1

Residual standard error: 0.07849 on 125 degrees of freedom
Multiple R-squared: 0.1403,    Adjusted R-squared: 0.1128
F-statistic: 5.102 on 4 and 125 DF,  p-value: 0.000768
```

Skewness + interactions

```
Coefficients:
                                Estimate Std. Error t value Pr(>|t|)
(Intercept)                     3.803854   0.007449 510.658  < 2e-16 ***
Latitude                        0.022997   0.009935   2.315 0.022421 *
Longitude                       0.024273   0.012168   1.995 0.048455 *
mean_temp                      -0.052191   0.017888  -2.918 0.004249 **
mean_precipitation              0.049405   0.018612   2.654 0.009079 **
prec_season                     0.012271   0.012507   0.981 0.328598
slope                          -0.020265   0.008376  -2.420 0.017120 *
sand                            0.009703   0.009521   1.019 0.310309
mean_temp:mean_precipitation    0.021378   0.007940   2.692 0.008163 **
mean_temp:prec_season           0.040736   0.010857   3.752 0.000278 ***
mean_temp:slope                -0.027401   0.014976  -1.830 0.069924 .
mean_precipitation:prec_season -0.033039   0.019377  -1.705 0.090906 .
mean_precipitation:slope       -0.034237   0.013392  -2.557 0.011884 *
mean_precipitation:sand        -0.026067   0.009597  -2.716 0.007634 **
prec_season:slope               0.024962   0.012810   1.949 0.053806 .
slope:sand                     -0.016495   0.010879  -1.516 0.132241
---
Signif. codes:  0 ‘***’ 0.001 ‘**’ 0.01 ‘*’ 0.05 ‘.’ 0.1 ‘ ’ 1

Residual standard error: 0.06998 on 114 degrees of freedom
Multiple R-squared: 0.3768,    Adjusted R-squared: 0.2948
```

Kurtosis

```
Coefficients:
                  Estimate Std. Error t value Pr(>|t|)
(Intercept)         2.0452     0.1022  20.012  < 2e-16 ***
Latitude            0.3887     0.1069   3.635 0.000405 ***
Longitude          -0.2122     0.1093  -1.942 0.054432 .
mean_temp           0.2376     0.1106   2.148 0.033655 *
mean_precipitation  0.4508     0.1128   3.996 0.000109 ***
---
Signif. codes:  0 ‘***’ 0.001 ‘**’ 0.01 ‘*’ 0.05 ‘.’ 0.1 ‘ ’ 1

Residual standard error: 1.165 on 125 degrees of freedom
Multiple R-squared: 0.3004,    Adjusted R-squared: 0.278
F-statistic: 13.42 on 4 and 125 DF,  p-value: 3.962e-09
```

Kurtosis + interactions

```
Coefficients:
                               Estimate Std. Error t value Pr(>|t|)
(Intercept)                     2.00532    0.10966  18.286  < 2e-16 ***
Latitude                        0.37655    0.13528   2.783  0.00627 **
Longitude                       0.19334    0.18138   1.066  0.28865
mean_temp                      -0.42288    0.23284  -1.816  0.07190 .
mean_precipitation              0.26573    0.17372   1.530  0.12879
prec_season                     0.25221    0.13617   1.852  0.06652 .
slope                          -0.01365    0.12354  -0.110  0.91220
sand                           -0.06738    0.13876  -0.486  0.62816
mean_temp:mean_precipitation    0.31956    0.12267   2.605  0.01038 *
mean_temp:prec_season           0.45421    0.15848   2.866  0.00493 **
mean_temp:sand                  0.21389    0.12607   1.697  0.09245 .
mean_precipitation:slope       -0.49243    0.20046  -2.456  0.01550 *
mean_precipitation:sand        -0.41305    0.16228  -2.545  0.01222 *
---
```

```
Signif. codes:  0 ‘***’ 0.001 ‘**’ 0.01 ‘*’ 0.05 ‘.’ 0.1 ‘ ’ 1

Residual standard error: 1.118 on 117 degrees of freedom
Multiple R-squared: 0.3968.    Adjusted R-squared: 0.3349
F-statistic: 6.413 on 12 and 117 DF.  p-value: 1.184e-08
```